Implementation of the Bethe–Salpeter Equation in the TURBOMOLE Program

Katharina Krause and Wim Klopper*

A software update solving the Bethe–Salpeter equation (BSE) is reported for the ESCF module of the TURBOMOLE program for the theoretical description of electronically excited states of atoms and molecules. A resolution-of-the-identity (RI) approximation is used for all two-electron electron-repulsion integrals that are required for solving the equation. Symmetry is utilized for the point group D_{2h} and its subgroups, and the BSE approach can be applied in either a spin-restricted or a spin-unrestricted Kohn–Sham formalism. Triplet as well as singlet excited states of closed-shell atoms and molecules can be treated in the spin-restricted formalism. As a side product, the present software update also allows for the application of the RI approximation to the Hartree–Fock exchange contribution that occurs when a hybrid functional is used in time-dependent density-functional theory. © 2016 Wiley Periodicals, Inc.

DOI: 10.1002/jcc.24688

Introduction

The computation of electronic excitation energies of atoms and molecules via the Bethe–Salpeter equation (BSE) has attracted considerable attention in recent years.[1–16] In the present Software News and Update, we report on the implementation of the BSE approach in the TURBOMOLE program[17] using a resolution-of-the-identity (RI) approximation for all two-electron electron-repulsion integrals that are required for solving the BSE.

The BSE approach can be applied to atoms and molecules for the theoretical description of electronically excited states in a very similar manner as the time-dependent density-functional-theory (TDDFT) approach, which is widely used in quantum chemistry. Accordingly, we have implemented the BSE approach in the ESCF module[18] of TURBOMOLE, which is the part of the program that is used for TDDFT calculations.

BSE calculations require quasiparticle energies on input. These quasiparticle energies can for example be obtained from *GW* calculations, which have recently been implemented (also in the ESCF module) in TURBOMOLE by Kaplan, van Setten, and coworkers.[19–22]

Technically speaking, BSE calculations are very similar to TDDFT calculations, and because in the software update we apply the RI approximation not only to the Coulomb terms (as has been done since many years) but also to the exchange terms, the new computer code not only enables efficient BSE calculations but also speeds up ordinary TDDFT calculations with hybrid functionals (and thus with Hartree–Fock-exchange contributions) significantly.

In the present article, we present the equations that have been implemented, some details on the algorithm, and a few numerical results. To ensure reproducibility, we report 32 singlet excitation energies for the molecules propenal, 1-phenylpyrrole, and 4-(dimethylamino)benzonitrile. To assess the performance of the BSE approach, we have computed 100 singlet excitation energies of 28 small organic molecules. Finally, CPU timings are reported for a set of five molecules ranging in size from benzene to pentacene.

Methods

Formalism

In the Bethe–Salpeter approach, just as in TDDFT, the following eigenvalue equation is solved,[23]

$$\begin{pmatrix} \mathbf{A} & \mathbf{B} \\ \mathbf{B}^* & \mathbf{A}^* \end{pmatrix} \begin{pmatrix} \mathbf{X}_n \\ \mathbf{Y}_n \end{pmatrix} = \omega_n \begin{pmatrix} \mathbf{1} & \mathbf{0} \\ \mathbf{0} & -\mathbf{1} \end{pmatrix} \begin{pmatrix} \mathbf{X}_n \\ \mathbf{Y}_n \end{pmatrix} \tag{1}$$

The electronically excited states are counted with the index n while ω_n is the corresponding excitation energy. We use a spin-orbital formalism with spin orbitals φ_p and corresponding energies ε_p. Usually, the spin orbitals φ_p are obtained from a Kohn–Sham computation while the energies ε_p are quasiparticle energies obtained from a many-body *GW* computation. In the following, the subscripts $i, j, k, \ldots$ refer to occupied spin orbitals, the subscripts $a, b, c, \ldots$ to virtual spin orbitals, and the subscripts $p, q, r, \ldots$ to the full set of spin orbitals.

The matrices **A** and **B** are defined as

$$A_{ia,jb} = \Delta\varepsilon_{ia,jb} + v_{ia,jb} - W_{ij,ab} \tag{2}$$

$$B_{ia,jb} = v_{ia,bj} - W_{ib,aj} \tag{3}$$

with

K. Krause, W. Klopper
Karlsruhe Institute of Technology (KIT), Institute of Physical Chemistry, P.O. Box 6980, Karlsruhe D-76049, Germany, E-mail: klopper@kit.edu

Contract grant sponsor: Deutsche Forschungsgemeinschaft (DFG) through SFB/TRR 88 "3MET" (Project No. C1)

$$\Delta\varepsilon_{ia,jb}=(\varepsilon_a-\varepsilon_i)\delta_{ij}\delta_{ab} \tag{4}$$

$$W_{pq,rs}=\sum_{tu}\left(\epsilon^{-1}\right)_{pq,tu}v_{tu,rs} \tag{5}$$

$$\varepsilon_{pq,rs}=\delta_{pr}\delta_{qs}-v_{pq,rs}[\chi_0(\omega=0)]_{rs,rs} \tag{6}$$

where δ_{tu} is the Kronecker delta. The elements of the diagonal matrix $\chi_0(\omega=0)$ are nonzero only for occupied−virtual pairs *kc* and virtual−occupied pairs *ck*,

$$[\chi_0(\omega=0)]_{kc,kc}=(\varepsilon_k-\varepsilon_c)^{-1} \tag{7}$$

$$[\chi_0(\omega=0)]_{ck,ck}=(\varepsilon_k-\varepsilon_c)^{-1} \tag{8}$$

The four-center two-electron integrals are given in Mulliken notation as

$$v_{pq,rs}=(qp|rs)=\int\int\varphi_q^*(1)\varphi_p(1)\frac{1}{r_{12}}\varphi_r^*(2)\varphi_s(2)\mathrm{d}\tau_1\mathrm{d}\tau_2 \tag{9}$$

Note that in the above formulation we have closely followed the notation used in section III. A of Ref. [23]. We refer to the work of Rebolini et al. for further details.[23]

RI approximation

In our implementation, the two-electron integrals of the Coulomb interaction $v_{pq,rs}$ and the static screened interaction $W_{pq,rs}$ are computed in the RI approximation,

$$v_{pq,rs}\approx\sum_P R_{qp,P}R_{P,rs} \tag{10}$$

$$W_{pq,rs}\approx\sum_{\tilde{P}\tilde{Q}}\tilde{R}_{qp,\tilde{P}}\left(\epsilon^{-1}\right)_{\tilde{P}\tilde{Q}}\tilde{R}_{\tilde{Q},rs} \tag{11}$$

The intermediate quantities $R_{P,rs}$ and $\tilde{R}_{\tilde{P},rs}$ are given by

$$R_{P,rs}=\sum_Q\left(\mathbf{v}^{-\frac{1}{2}}\right)_{PQ}(Q|rs) \tag{12}$$

$$v_{PQ}=(P|Q) \tag{13}$$

$$\tilde{R}_{\tilde{P},rs}=\sum_{\tilde{Q}}\left(\mathbf{v}^{-\frac{1}{2}}\right)_{\tilde{P}\tilde{Q}}\left(\tilde{Q}|rs\right) \tag{14}$$

$$v_{\tilde{P}\tilde{Q}}=\left(\tilde{P}|\tilde{Q}\right) \tag{15}$$

while the matrix elements of ϵ are computed from the expression

$$\epsilon_{\tilde{P}\tilde{Q}}=\delta_{\tilde{P}\tilde{Q}}-\chi_{\tilde{P}\tilde{Q}} \tag{16}$$

$$\chi_{\tilde{P}\tilde{Q}}=2\Re\sum_{kc}\tilde{R}_{\tilde{P},kc}(\varepsilon_k-\varepsilon_c)^{-1}\tilde{R}_{kc,\tilde{Q}} \tag{17}$$

In the above equations, two distinct auxiliary basis sets $\{\varphi_P\}$ and $\left\{\varphi_{\tilde{P}}\right\}$ are used, but in actual computations, these basis sets can of course be chosen to be equal. The auxiliary basis sets are real.

In Mulliken notation, the three- and two-center two-electron integrals are given as

$$(Q|rs)=\int\int\varphi_Q(1)\frac{1}{r_{12}}\varphi_r^*(2)\varphi_s(2)\mathrm{d}\tau_1\mathrm{d}\tau_2 \tag{18}$$

$$(\mathrm{P}|Q)=\int\int\varphi_P(1)\frac{1}{r_{12}}\varphi_Q(2)\mathrm{d}\tau_1\mathrm{d}\tau_2 \tag{19}$$

Implementation

Auxiliary basis sets

As already shown in the previous subsection, our implementation in the TURBOMOLE program[17] relies on the RI approximation, which makes the code very efficient. For the Coulomb interaction $v_{pq,rs}$, the RI approximation is invoked by introducing the (optional) keyword \$rij and providing an auxiliary basis set ("jbas," $\{\varphi_P\}$). For the static screened interaction $W_{pq,rs}$, the RI approximation is invoked by introducing the (mandatory) keyword \$rik and providing an auxiliary basis set ("cbas," $\left\{\varphi_{\tilde{P}}\right\}$). Two different auxiliary basis sets ("jbas" and "cbas") can be used for the two interactions, but we recommend to use only the "cbas" auxiliary basis set $\left\{\varphi_{\tilde{P}}\right\}$ as one single set for all RI approximations. (To do this, however, the user must edit the file that contains the auxiliary basis sets and make sure that the "jbas" and "cbas" sets are identical; of course, also the "jbas" auxiliary basis sets can be used for all RI approximations by manipulating the auxiliary-basis-set input file accordingly.) With respect to this point, we note that the "cbas" auxiliary basis sets have been optimized for approximating integrals of the type $(ai|bj)$, which are the integrals that occur in the matrices **A** and **B**.

In our TURBOMOLE implementation, the Coulomb interaction $v_{pq,rs}$ can be computed either with or without auxiliary basis set, whereas the static screened interaction $W_{pq,rs}$ can only be computed using the RI approximation.

Static screened interaction

We define a Coulomb matrix **v** with matrix elements $v_{pq,rs}=(qp|rs)$. Then, in terms of the matrix $\boldsymbol{R}$ with elements $R_{P,rs}$, we can write the RI approximation in matrix form as

$$\mathbf{v}\approx\mathbf{R}^\top\mathbf{R} \tag{20}$$

Analogously, for the screened exchange interaction, the RI approximation takes the form

Table 1. Cartesian coordinates (in Å) of propenal.

Atom	*x*	*y*	*z*
C	−0.152147	−0.739760	0.000000
O	−1.211340	−1.314465	0.000000
H	0.804971	−1.304092	0.000000
C	0.000000	0.719700	0.000000
C	1.209076	1.272423	0.000000
H	−0.911266	1.307850	0.000000
H	1.354992	2.345216	0.000000
H	2.100449	0.652565	0.000000

Table 2. BSE excitation energies (in eV) of propenal.

A'	A''
7.054	3.763
9.230	7.560
9.592	8.142
9.720	8.388

$$\mathbf{W} \approx \tilde{\mathbf{R}}^{\top}\epsilon^{-1}\tilde{\mathbf{R}} = \tilde{\mathbf{R}}^{\top}\bar{\epsilon}\tilde{\mathbf{R}} = \tilde{\mathbf{R}}^{\top}\bar{\mathbf{R}} = \bar{\mathbf{R}}^{\top}\tilde{\mathbf{R}} \tag{21}$$

Here, we have introduced $\bar{\mathbf{R}} = \bar{\epsilon}\tilde{\mathbf{R}}$ and $\bar{\epsilon} = \epsilon^{-1}$. In our implementation, the latter can be computed either by means of a Cholesky decomposition of ϵ (this technique is set as default) or by means of the iterative procedure

$$\bar{\epsilon}^{(i+1)} = \mathbf{1} + \chi\bar{\epsilon}^{(i)} \tag{22}$$

with $\bar{\epsilon}^{(0)} = \mathbf{1}$.

Subspace iterations

The TDDFT and BSE are usually solved for a limited number of low eigenvalues by means of a subspace method that avoids the explicit construction of the matrices **A** and **B**. In this method, the products of these matrices with a trial vector **Z** are computed. For the screened exchange contributions of the BSE approach, the corresponding matrix−vector products have been implemented as follows:

$$\sigma^{\mathbf{A}}_{ia}(\mathbf{Z}) = -\sum_{jb} W_{ij,ab}Z_{jb} = -\sum_{\tilde{Q}j} \bar{R}_{ji,\tilde{Q}} \left(\sum_{b} \tilde{R}_{\tilde{Q},ab}Z_{jb} \right) \tag{23}$$

$$\sigma^{\mathbf{B}}_{ia}(\mathbf{Z}) = -\sum_{jb} W_{ib,aj}Z_{jb} = -\sum_{\tilde{Q}j} \bar{R}_{\tilde{Q},aj} \left(\sum_{b} \tilde{R}_{bi,\tilde{Q}}Z_{jb} \right) \tag{24}$$

Results

Test cases

In this subsection, we report excitation energies for the molecules propenal (also known as acrolein), 1-phenylpyrrole, and 4-(dimethyl-amino)benzonitrile (DMABN), computed with the TURBOMOLE program using the BSE approach, the PBE0 functional,[24] and the 6-311G* basis set.[25] The purpose of reporting these energies is to present energies of a few simple test cases that can easily be reproduced by other computer implementations of the BSE approach. The molecular geometries were kept fixed. The geometry of propenal is given in Table 1 while the geometries of 1-phenylpyrrole and DMABN were taken from Ref. [26].

Table 3. BSE excitation energies (in eV) of 1-phenylpyrrole.

A_1	A_2	B_1	B_2
5.316	7.153	7.357	5.055
6.071	7.840	7.717	**5.343**
6.435	7.927	7.820	6.552
6.995	8.051	8.054	7.070

The values printed in bold type refer to the two charge-transfer excitations studied in Ref. [26].

Table 4. BSE excitation energies (in eV) of DMABN.

A'	A''
4.813	4.559
6.191	5.483
6.507	5.904
6.637	5.959

The value printed in bold type refers to the charge-transfer excitation studied in Ref. [26].

The computation with TURBOMOLE was performed using the "universal" Coulomb-fitting auxiliary basis sets for H, C, N, and O from Ref. [27]. These auxiliary basis sets were used for all RI approximations (Coloumb and static screened exchange). The quasiparticle energies required for the BSE computation were generated by shifting all PBE0/6-311G* virtual orbital energy levels by 5.4904 eV in the case of propenal, by 3.8811 eV in the case of 1-phenylpyrrole, and by 3.5956 eV in the case of DMABN to higher values (these shifts were obtained from *GW* calculations with the FIESTA program[28–30]). Tables 2–4 show the computed BSE excitation energies.

All energies presented in Tables 2–4 agree with the corresponding energies computed with the FIESTA program[28–30] (with the same orbital basis and auxiliary basis sets) to within a median absolute deviation of 0.1 meV. The root-mean-square deviation amounts to 0.3 meV. The energies are plotted in Figure 1.

Peach et al.[26] report a reference value of 4.56 eV for the 2 $^1A'$ charge-transfer state of DMABN. Our BSE value of 4.81 eV is 0.25 eV larger but in rather good agreement with Peach's CAM-B3LYP value of 4.91 eV. Figure 2 displays the transition density of this charge-transfer excitation. Its

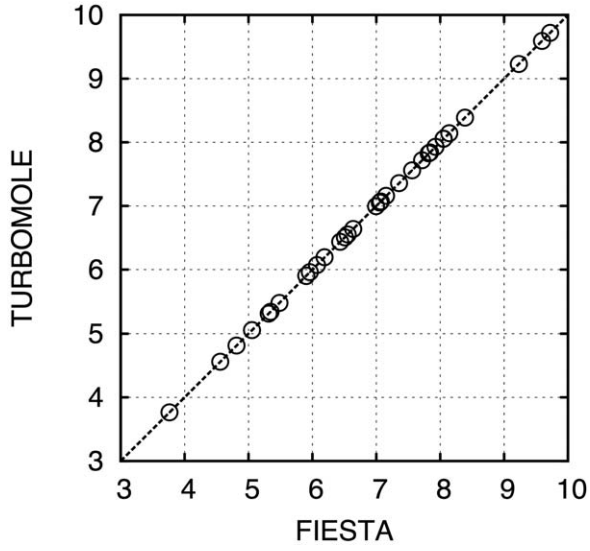

Figure 1. The excitation energies (in eV) displayed in Tables 2–4, which were computed with the TURBOMOLE program, are plotted against the corresponding excitation energies computed with the FIESTA program.

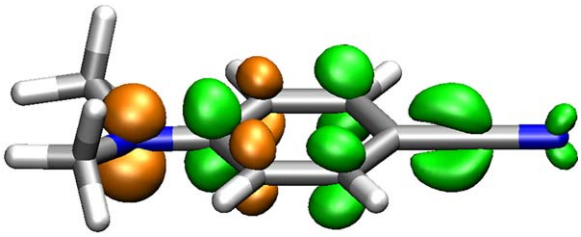

Figure 2. Transition density of the excitation at 4.813 eV of DMABN. Green corresponds to a gain of electron density while orange corresponds to a loss of electron density (iso-value: 0.005 a_0^{-3}). [Color figure can be viewed at wileyonlinelibrary.com]

charge-transfer diagnostic[26] Λ amounts to 0.75, which in the present work is computed from the spatial overlap of the dominating particle/hole pair of (real) natural transition orbitals (NTOs),

$$\Lambda = \int \left| \phi^{\mathrm{NTO}}_{\mathrm{hole}}(\mathbf{r}) \phi^{\mathrm{NTO}}_{\mathrm{particle}}(\mathbf{r}) \right| \mathrm{d}\mathbf{r} \tag{25}$$

For the 2 $^1B_2$ and 3 $^1A_1$ charge-transfer excitations of 1-phenylpyrrole, Peach et al.[26] report reference values of 5.47 and 5.94 eV. Our BSE values of 5.34 and 6.07 eV agree well with these reference values, indicating that the BSE approach is able to describe charge-transfer excitations. In Figure 3, we plot the dominating particle/hole pairs of NTOs of the two states. The corresponding charge-transfer diagnostics amount to $\Lambda =$ 0.62 (2 $^1B_2$) and $\Lambda =$ 0.20 (3 $^1A_1$). The charge-transfer character of the 3 $^1A_1$ state is particularly pronounced. In the course of this excitation, charge is transferred from the pyrrole ring, where the hole NTO resides, to the phenyl ring, where the particle NTO resides (cf., Fig. 3).

CPU timings

For the molecules benzene (**1**), naphthalene (**2**), anthracene (**3**), tetracene (**4**), and pentacene (**5**), Table 5 shows CPU timings for the calculation of 40 excited singlet states in the def2-TZVP basis.[31] TURBOMOLE's grid 4 was used and the convergence threshold was set to rpaconv = 6. Five excited states were computed in each of the eight irreducible representations (irreps) of the D_{2h} point group. The def2-TZVP "cbas" auxiliary basis,[32] which has been optimized for RI-MP2* calculations in the def2-TZVP orbital basis, was used for all RI approximations. Timings for the BSE computations are compared with those for solving the TDDFT equations using the functionals PBE[33] and PBE0.[24] The BSE calculations used quasiparticle energies obtained from an x_α-G_0W_0 calculation[34] with $\alpha = 0.703$ and 0.622 for the PBE and PBE0 functionals, respectively.

Table 5 shows that the timings for the BSE calculations as well as for the TDDFT calculations with the PBE0 hybrid functional are of the same order of magnitude as for the TDDFT calculations with the generalized gradient approximation (GGA) functional PBE. Only for the largest of the five systems, pentacene, the BSE calculations were 4–5 times more time consuming than the GGA-TDDFT calculation in the RI approximation.

*Method based on second-order Møller–Plesset perturbation theory, implemented using a resolution-of-the-identity approximation.

Table 5. CPU timings (in minutes:seconds) for the computation of 40 singlet excitation energies (5 in each irrep of D_{2h}) of benzene (**1**), naphthalene (**2**), anthracene (**3**), tetracene (**4**), and pentacene (**5**), measured in the def2-TZVP basis on a single Intel® Xeon® X5650 (12M Cache, 2.66 GHz) processor.

	PBE/DFT	PBE/BSE	PBE0/DFT	PBE0/BSE
1	1:54 (7)	1:30 (10)	3:22 (8)	1:34 (10)
2	5:21 (8)	6:27 (13)	11:04 (9)	6:22 (13)
3	10:09 (8)	19:34 (13)	25:35 (9)	20:07 (13)
4	15:31 (8)	42:11 (12)	58:35 (11)	45:38 (13)
5	20:54 (9)	86:14 (13)	100:07 (9)	92:50 (13)

The number of iterations is given in parentheses.

It is worth noting that without invoking any RI approximations, the TDDFT calculation on pentacene with the PBE0 hybrid functional took 9 h and 39 min. The computing time was somewhat reduced by applying the RI approximation to the Coulomb interaction (7 h and 33 min), but only after applying the RI approximation also to the Hartree–Fock exchange part of the hybrid functional, the computation time was reduced to as short as 1 h and 40 min (cf., Table 5). Hence, computing the (static screened) exchange contribution in the RI approximation speeded up the calculation by about a factor of five.

Performance

Similarly to what was done in Ref. [4], we have computed singlet excitation energies using the BSE approach for the test set of Ref. [35]. This test set comprises 28 small organic molecules with theoretical best estimates (TBE) for 104 singlet excitation energies. We have disregarded the 1 $^1B_{3g}$ state of *s*-tetrazine as well as the 2 ^1A_g states of butadiene, hexatriene, and octatetraene, which are states of "doubly-excited character." Thus, 100 excitation energies of the test set were analyzed by comparing the computed energies with the TBE-2 values of Ref. [35]. The geometries were taken from Ref. [36]. These were kept fixed.

We have not only applied the BSE and TDDFT approaches (using the PBE0 functional) but also the CC2[37] approach as implemented in the RICC2 module[38] of the TURBOMOLE program.[17] These CC2 calculations were carried out in the same def2-TZVP basis (and auxiliary basis) as used in the BSE calculations, but in contrast to the BSE calculations, the 1s core orbitals of C, N, and O were kept frozen in the CC2 calculations (frozen-core approximation).

The quasiparticle energies for the BSE approach were either obtained from x_α-G_0W_0 or from G_0W_0 calculations and we refer to the corresponding results as x_α-G_0W_0-BSE and G_0W_0-BSE in the following. In the G_0W_0 calculations, we restricted the prefactor Z_p in eq. (4) of Ref. 34 to values between 0 and 1. We applied the PBE0 functional for the x_α-G_0W_0-BSE, G_0W_0-BSE, and TDDFT calculations. The parameter $\alpha = 0.651$ was determined by minimizing the root-mean-square deviation from the

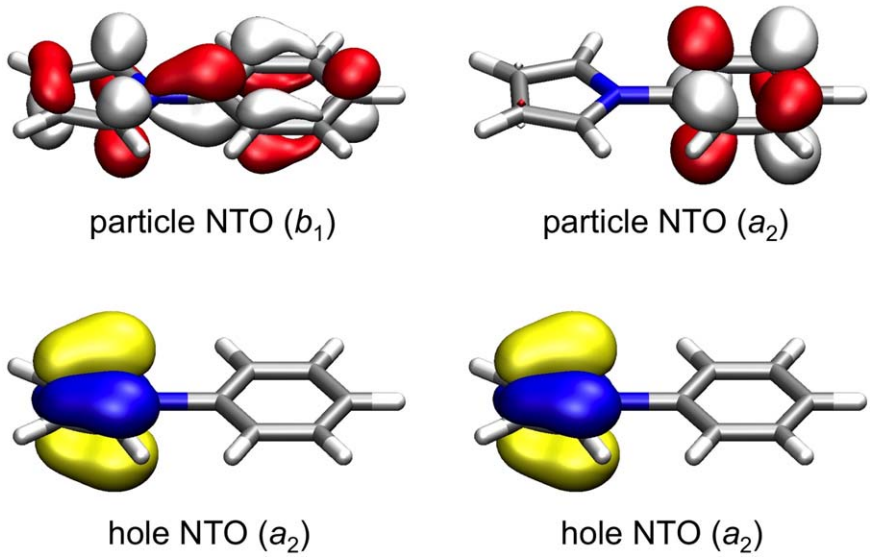

Figure 3. Dominating particle/hole pairs of NTOs of the excitations at 5.343 eV (left pair) and 6.071 eV (right pair) of 1-phenylpyrrole (iso-value: 0.05 a_0^{-3}). [Color figure can be viewed at wileyonlinelibrary.com]

reference values. Note that in the x_α-G_0W_0 approach, only exchange contributions are computed. In this approach,[34] the quasiparticle energy ε_p is obtained by adding the difference between the exchange self-energy Σ_X and the exchange potential V_X (scaled by an empirically optimized parameter α) to the Kohn−Sham orbital energy ε_p^{KS},

$$\varepsilon_p = \varepsilon_p^{KS} + \alpha\langle\varphi_p|\Sigma_X - V_X|\varphi_p\rangle \quad (26)$$

The TDDFT and CC2 excitation energies are plotted against the TBE-2 values in Figure 4 while the x_α-G_0W_0-BSE and G_0W_0-BSE energies are plotted in Figure 5. Table 6 shows the statistical analysis of the deviations of the computed excitation energies from the TBE-2 values.

Figures 4 and 5 as well as the statistical analysis presented in Table 6 show clearly that the performance of the BSE approach is not as good as the performance of the TDDFT and CC2 methods. In agreement with the study reported in Ref. [4], we find that the G_0W_0-BSE excitation energies are too small on average. The x_α-G_0W_0-BSE energies are more evenly distributed about the TBE-2 reference values, but the spread of the distribution is larger than for the TDDFT and CC2 results. Anyway, the results presented here are only preliminary and a more thorough performance assessment of the BSE approach would be desirable. Such an assessment would for example address a large variety of functionals, basis sets, and *GW* methods. It may also be worthwhile to investigate which set of Kohn−Sham orbital energy levels should be corrected

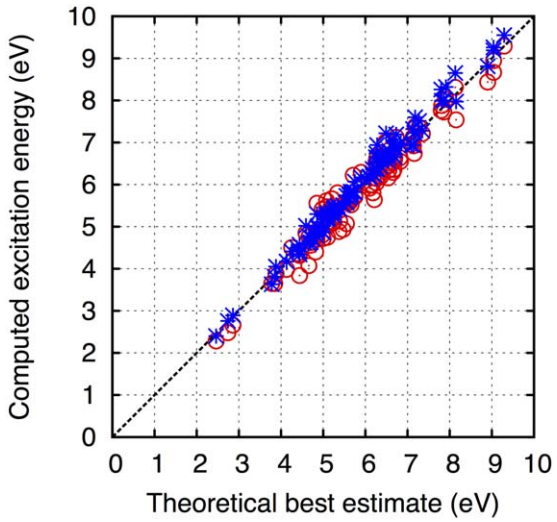

Figure 4. TDDFT (red circles, computed at the PBE0/def2-TZVP level) and CC2/def2-TZVP (blue stars) excitation energies plotted against the theoretical best estimates (TBE-2 values) of Ref. [36]. [Color figure can be viewed at wileyonlinelibrary.com]

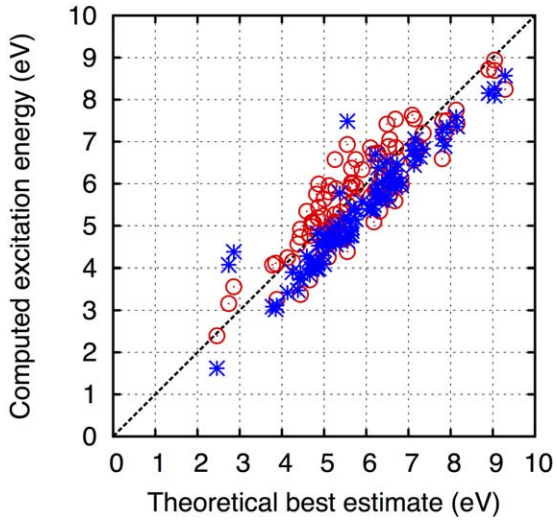

Figure 5. Computed x_α-G_0W_0-BSE (red circles) and G_0W_0-BSE (blue stars) excitation energies plotted against the theoretical best estimates (TBE-2 values) of Ref. [36]. Computed at the PBE0/def2-TZVP level. [Color figure can be viewed at wileyonlinelibrary.com]

Table 6. Statistical analysis in terms of mean deviation (DEV), mean absolute deviation (ABS), maximum absolute deviation (MAX), root-mean-square deviation (RMS), and median absolute deviation (MAD).

	x_α-G_0W_0-BSE	G_0W_0-BSE	TDDFT	CC2
DEV	−0.04	−0.50	−0.06	0.13
ABS	0.50	0.61	0.22	0.16
MAX	1.37	1.94	0.71	0.73
RMS	0.59	0.67	0.28	0.21
MAD	0.23	0.15	0.10	0.06

All values in eV.

or shifted when generating the quasiparticle energies for the BSE calculation. Furthermore, the BSE approach may outperform the TDDFT approach for states with multiple-excitation or charge-transfer character, as for example occurring in transition-metal complexes. It remains to be seen whether the BSE approach could be a useful tool for the study of cooperative effects in electronic spectra of oligonuclear transition-metal complexes.[39]

Conclusions

The BSE approach has been implemented in the TURBOMOLE program. The implementation is efficient due to the application of RI approximations to all two-electron electron-repulsion integrals (Coulomb and exchange). As a side product, the implementation also allows for the application of the RI approximation to the Hartree−Fock exchange contribution in standard TDDFT calculations.

Only preliminary results are presented in the present article and a more thorough assessment of the BSE approach, in particular with respect to applications to transition-metal compounds, would be desirable.

Acknowledgment

We thank Jing Li and Xavier Blase (Institut Néel, Grenoble) for giving us access to the FIESTA program.

Keywords: electronic excitation energy · time-dependent density-functional theory · Bethe−Salpeter equation · resolution-of-the-identity approximation · exchange interaction

How to cite this article: K. Krause, W. Klopper. *J. Comput. Chem.* **2017**, *38*, 383–388. DOI: 10.1002/jcc.24688

[1] D. Jacquemin, I. Duchemin, X. Blase, *Mol. Phys.* **2016**, *114*, 957.
[2] X. Blase, P. Boulanger, F. Bruneval, M. Fernandez-Serra, I. Duchemin, *J. Chem. Phys.* **2016**, *144*, 034109.
[3] D. Jacquemin, I. Duchemin, X. Blase, *J. Chem. Theory Comput.* **2015**, *11*, 5340.
[4] D. Jacquemin, I. Duchemin, X. Blase, *J. Chem. Theory Comput.* **2015**, *11*, 3290.
[5] S. Körbel, P. Boulanger, I. Duchemin, X. Blase, M. A. L. Marques, S. Botti, *J. Chem. Theory Comput.* **2014**, *10*, 3934.
[6] B. Baumeier, M. Rohlfing, D. Andrienko, *J. Chem. Theory Comput.* **2014**, *10*, 3104.
[7] B. Baumeier, D. Andrienko, M. Rohlfing, *J. Chem. Theory Comput.* **2012**, *8*, 2790.
[8] B. Baumeier, D. Andrienko, Y. Ma, M. Rohlfing, *J. Chem. Theory Comput.* **2012**, *8*, 997.
[9] J. M. Garcia-Lastra, K. S. Thygesen, *Phys. Rev. Lett.* **2011**, *106*, 187403.
[10] A. M. Conte, L. Guidoni, R. Del Sole, O. Pulci, *Chem. Phys. Lett.* **2011**, *515*, 290.
[11] D. Rocca, D. Lu, G. Galli, *J. Chem. Phys.* **2010**, *133*, 164109.
[12] Y. Ma, M. Rohlfing, C. Molteni, *Phys. Rev. B* **2009**, *80*, 241405.
[13] M. Palummo, C. Hogan, F. Sottile, P. Balagá, A. Rubio, *J. Chem. Phys.* **2009**, *131*, 084102.
[14] M. L. Tiago, J. R. Chelikowsky, *Phys. Rev. B* **2006**, *73*, 205334.
[15] J. C. Grossman, M. Rohlfing, L. Mitas, S. G. Louie, M. L. Cohen, *Phys. Rev. Lett.* **2001**, *86*, 472.
[16] M. Rohlfing, S. G. Louie, *Phys. Rev. B* **2000**, *62*, 4927.
[17] F. Furche, R. Ahlrichs, C. Hättig, W. Klopper, M. Sierka, F. Weigend, *WIREs Comput. Mol. Sci.* **2014**, *4*, 91.
[18] F. Furche, D. Rappoport, In Theoretical and Computational Chemistry, Vol. 16: Computational Photochemistry; M. Olivucci, Ed.; Elsevier: Amsterdam, **2005**; p. 93.
[19] F. Kaplan, M. E. Harding, C. Seiler, F. Weigend, F. Evers, M. J. van Setten, *J. Chem. Theory Comput.* **2016**, *12*, 2528.
[20] M. J. van Setten, F. Caruso, S. Sharifzadeh, X. Ren, M. Scheffler, F. Liu, J. Lischner, L. Lin, J. R. Deslippe, S. G. Louie, C. Yang, F. Weigend, J. B. Neaton, F. Evers, P. Rinke, *J. Chem. Theory Comput.* **2015**, *11*, 5665.
[21] F. Kaplan, F. Weigend, F. Evers, M. J. van Setten, *J. Chem. Theory Comput.* **2015**, *11*, 5152.
[22] M. J. van Setten, F. Weigend, F. Evers, *J. Chem. Theory Comput.* **2013**, *9*, 232.
[23] E. Rebolini, J. Toulouse, A. Savin, In *Concepts and Methods in Modern Theoretical Chemistry: Electronic Structure and Reactivity*; S. K. Ghosh, P. K. Chattaraj, Eds.; CRC Press: Boca Raton, **2013**; p. 367.
[24] J. P. Perdew, M. Ernzerhof, K. Burke, *J. Chem. Phys.* **1996**, *105*, 9982.
[25] R. Krishnan, J. S. Binkley, R. Seeger, J. A. Pople, *J. Chem. Phys.* **1980**, *72*, 650.
[26] M. J. G. Peach, P. Benfield, T. Helgaker, D. J. Tozer, *J. Chem. Phys.* **2008**, *128*, 044118.
[27] F. Weigend, *Phys. Chem. Chem. Phys.* **2006**, *8*, 1057.
[28] X. Blase, C. Attaccalite, V. Olevano, *Phys. Rev. B* **2011**, *83*, 115103.
[29] X. Blase, C. Attaccalite, *Appl. Phys. Lett.* **2011**, *99*, 171909.
[30] I. Duchemin, P. Boulanger, X. Blase, FIESTA program, a Gaussian-based *GW*/BSE code.
[31] F. Weigend, R. Ahlrichs, *Phys. Chem. Chem. Phys.* **2005**, *7*, 3297.
[32] F. Weigend, M. Häser, H. Patzelt, R. Ahlrichs, *Chem. Phys. Lett.* **1998**, *294*, 143.
[33] J. P. Perdew, K. Burke, M. Ernzerhof, *Phys. Rev. Lett.* **1996**, *77*, 3865.
[34] K. Krause, M. E. Harding, W. Klopper, *Mol. Phys.* **2015**, *113*, 1952.
[35] M. R. Silva-Junior, M. Schreiber, S. P. A. Sauer, W. Thiel, *J. Chem. Phys.* **2010**, *133*, 174318.
[36] M. Schreiber, M. R. Silva-Junior, S. P. A. Sauer, W. Thiel, *J. Chem. Phys.* **2008**, *128*, 134110.
[37] O. Christiansen, H. Koch, P. Jørgensen, *Chem. Phys. Lett.* **1995**, *243*, 409.
[38] C. Hättig, F. Weigend, *J. Chem. Phys.* **2000**, *113*, 5154.
[39] J. Chmela, M. E. Harding, D. Matioszek, C. E. Anson, F. Breher, W. Klopper, *ChemPhysChem* **2016**, *17*, 37.

Received: 28 September 2016
Revised: 15 November 2016
Accepted: 17 November 2016
Published online on 7 December 2016